RSC Advances

PAPER

View Article Online
View Journal | View Issue

Cite this: *RSC Adv.*, 2026, **16**, 16687

Bidentate bis(NHC-carboxylate) palladium and nickel complexes for the hydrosilylative reduction of carbonyl compounds

Jorge Sanz-Garrido, [a] Carlos J. Carrasco, [b] Camino Gonzalez-Arellano, [a] Francisco Montilla, [b] Agustín Galindo *[b] and Juan C. Flores *[a]

A family of 16 e$^-$ Pd(II) and Ni(II) biscarbenes bearing NHC ligands decorated with different amino acids in the side chain has been synthesized. The Pd complexes were accessible through transmetalation with silver carbenes generated *in situ*, while the Ni species were obtained by deprotonation of the imidazolium salt with LDA, followed by complete ligand substitution in [$NiBr_2$(dme)]. The new complexes have been studied as catalysts in the reductive hydrosilylation of aldehydes and ketones with phenylsilane, followed by a hydrolysis step to form the corresponding alcohol. One of the nickel biscarbene complexes proved to be a competent catalyst, in which the presence of the carboxylate moieties appears to be beneficial. A DFT study of the electronic and steric properties of NHC-carboxylate ligands has been carried out to identify the key features of the complex that exhibits the highest catalytic activity.

Received 6th January 2026
Accepted 16th March 2026

DOI: 10.1039/d6ra00132g

rsc.li/rsc-advances

Introduction

Over the last decades, *N*-heterocyclic carbene (NHC) ligands have attracted great attention across many fields of chemistry,[1] particularly in organometallic chemistry, where they play a central role in a wide variety of complexes.[2] This family of ligands is useful due to the robust metal–carbon bond they form thanks to their extraordinary σ-donor capability and the steric protection provided by their *N*-substituents, together the versatility and tunability of their structure. Given these features, it is not surprising that many NHC complexes have found applications as excellent catalysts in a variety of organic transformations.[3]

As with any family of ligands, chiral versions of NHCs are attractive for accessing the synthesis of enantiopure complexes, which may have applications in asymmetric catalysis.[4] To that end, the presence of a bidentate (or polydentate) NHC ligand would prevent the metal–carbon rotation, thereby ensuring the retention of the steric information in the close proximity to the metal.[5]

Complexes containing κ^2-C,O-NHC-carboxylate chelating ligands from group 10 are scarce. To the best of our knowledge, there are only two examples of palladium complexes of this type. One is a biscarbene described by Danopoulos and coworkers in 2008,[6] and the other is a group of amino acid derived chiral biscarbenes that we have described more recently (Chart 1).[7]

Nickel complexes containing κ^2-C,O chelating NHC ligands also remain largely unexplored, with only a few examples reported. Shen and coworkers have synthesized biscarbene complexes bearing phenolate-tethered NHC chelating ligands.[8] Later, the group of Heinicke described one such complex with an enolate moiety.[9] In 2020, Bertini and Albrecht reported a series of phenolate-substituted mesoionic and normal carbene complexes similar to those prepared by Shen.[10] Finally, we have also described a biscarbene complex of this type (Chart 1).[7]

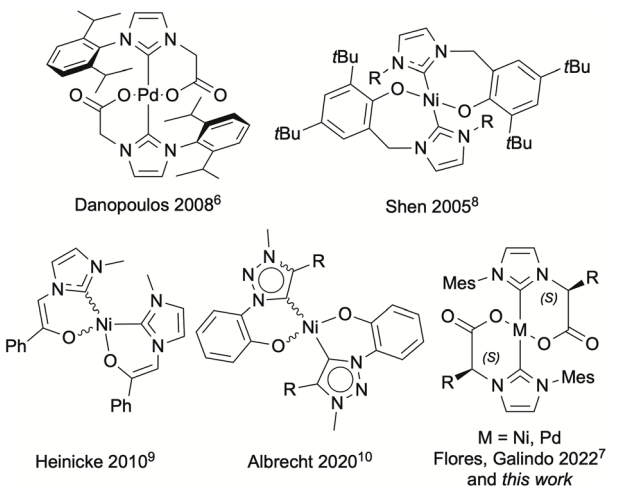

Chart 1 .

[a]*Departamento de Química Orgánica y Química Inorgánica, Instituto de Investigación Química "AndrésM. del Río", Universidad de Alcalá, Ctra. A-2, Km. 33,600, Madrid, 28805, Spain. E-mail: juanc.floresuah.es*

[b]*Departamento de Química Inorgánica, Facultad de Química, Universidad de Sevilla, Aptdo 1203, Sevilla, 41071, Spain. E-mail: galindo@us.es*

We report here new bis(NHC-carboxylate) palladium and nickel complexes derived from amino acids and their catalytic performances in the hydrosilylation of different aldehydes and ketones. The theoretical analysis of the electronic and steric features of NHC-carboxylate ligands has enabled the identification of several factors that account for the superior catalytic activity of one of the nickel complexes.

Results and discussion

Synthesis of metal complexes

The NHC palladium complexes previously described (Chart 1) were derived from the amino acids L-alanine, L-valine and L-leucine (R = Me, ^{i}Pr, ^{i}Bu, respectively).[7] Their synthesis is feasible through the formation of a silver carbene species and subsequent transmetalation with an appropriate Pd source. Alternatively, the carbene can be generated *in situ* through the corresponding acid–base deprotonation reaction, followed by a ligand exchange process with $Pd(OAc)_2$. The new complexes reported herein have been prepared following the first method (Scheme 1). Thus, syntheses using imidazolium proligands derived from L-isoleucine and L-phenylalanine have enabled the isolation of the corresponding biscarbene complexes, **ILe$_2$Pd** and **Phe$_2$Pd**. These complexes were obtained as light brown solids in modest yields and were found to be stable exposed to air.

The ^{1}H and $^{13}C\{^{1}H\}$ NMR spectra of the palladium complexes exhibit the characteristic resonances of the imidazolylidene C–H moieties at 7–6.2 ppm and 121 ppm, respectively. The carbene carbon resonates at 164 ppm, which is within the normal range for this kind of compounds.

Analogous Ni biscarbene complexes are known to form as byproducts in the synthesis of the half-sandwich related compounds with general formula **AANiCp**, in reactions that can be driven to favor the formation of the biscarbene metal compound under certain conditions.[11] However, a more straightforward synthetic method with an easier isolation protocol would be desirable. The reaction *via* transmetalation under the same conditions as those for synthesizing the palladium counterparts (*i.e.*, through silver carbene intermediates) did not furnish the desired product. We have already described that the deprotonation of the imidazolium salt derived from L-valine with LDA and *in situ* complexation of the resulting carbene with $[NiBr_2(dme)]$ (dme = dimethoxyethane) is a suitable procedure for the preparation of **Val$_2$Ni**.[7] The same pathway also worked with the proligands derived from L-leucine, L-isoleucine and L-phenylalanine, allowing the isolation of the corresponding **AA$_2$Ni** biscarbene compounds (Scheme 2), but failed when using the imidazolium salt derived from L-alanine.

The alanine-derived Ni biscarbene compound could only be detected by ^{1}H NMR in small quantities in the crude of the reaction, but isolation in a pure form was unattainable, observing decomposition in all attempts tested. We believe that this instability could be due to the smaller size of the substituent on the stereo-genic carbon (R = Me), which must provide insufficient steric protection to the metal center. In contrast, the nickel complexes substituted with leucine, isoleucine and phenylalanine moieties were found to be stable yellow solids that remain unchanged in air for months.

Catalytic hydrosilylative reduction of carbonyl compounds

Inspired by the extraordinary activity observed by Bertini and Albrecht in the hydrosilylative reduction of aldehydes with the related biscarbene complexes of nickel $[(\kappa^2\text{-C,O-NHC})_2Ni]$ (Chart 1),[10] the catalytic study in this reaction began with benzaldehyde as the substrate (step 1 in Scheme 3). The leucine-derived biscarbene complexes **Leu$_2$M** (M = Ni, Pd) were chosen as catalysts because previous results in other transformations showed that **Leu** catalysts outperform those derived from other amino acids.[11,12] In the reaction with benzaldehyde, the Ni complex proved to be a superior catalyst, delivering the expected product with complete conversion. In contrast, 69% of the aldehyde was converted to the corresponding alcohol with the palladium catalyst under the conditions summarized in Scheme 3.

We have also conducted the reaction catalyzed by **Leu$_2$Ni** with three other substrates (Chart 2). The reaction resulted to be sensitive to the nature of the *para*-substituent in the ring. The more electron-deficient *p*-bromobenzaldehyde underwent complete conversion, while it dropped to 61% for the electron-rich *p*-methoxy substituted compound. Under the same conditions, the conjugated substrate cinnamaldehyde could also be completely reduced, in a reaction with total chemoselectivity toward the allylic alcohol (**2d**).

Although **Leu$_2$Ni** seems to be less effective in the formation of **2a–c** than the mesoionic complexes described by Albrecht,

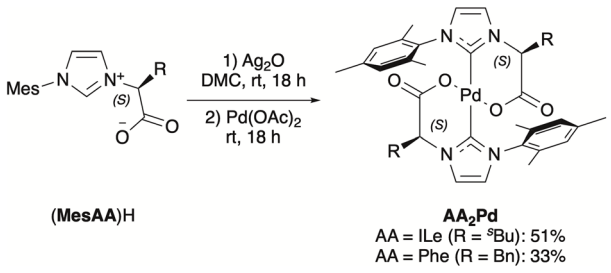

Scheme 1 Synthesis of the Pd biscarbene complexes through transmetalation.

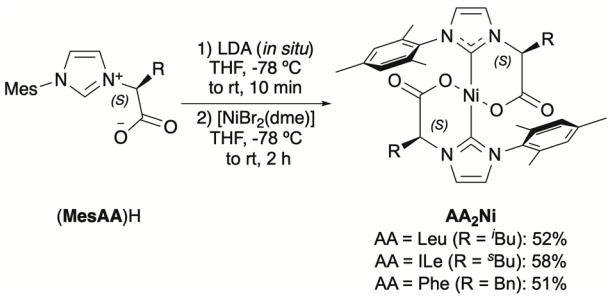

Scheme 2 Synthesis of the Ni biscarbene complexes through deprotonation and *in situ* complexation.

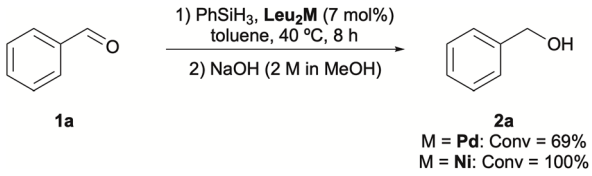

Scheme 3 Hydrosilylative reduction of benzaldehyde (**1a**) catalyzed by Leu_2Ni or Leu_2Pd.

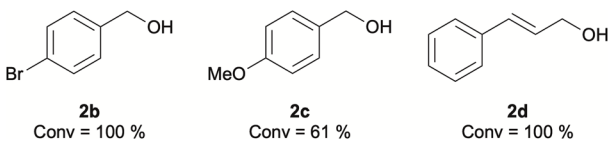

Chart 2 .

the latter are much less active with the bromide than with the methoxy derivative.[10] Nevertheless, the most significant difference is observed in the reaction with ketones, which are less reactive substrates. The AA_2M (M = Ni, Pd) complexes are able to react with ketones, whereas the triazolylidene complexes are reported to be inactive. Acetophenone was used as a model substrate for the initial optimization of the reaction conditions (Table 1). Compared with Leu_2Pd, the nickel biscarbene delivered better outcomes at 50 °C in THF or in toluene (Table 1, entries 2, 4 *vs.* 6, 8) achieving conversions of up to 91%. Having established that the Leu_2Ni complex performs better than the Pd analogous in this reaction as well, we continued the optimization of conditions only with the nickel complexes. Toluene demonstrated to be the best of the solvents tested (Table 1, entries 8 *vs.* 6, 9, 10, 11, 12). The biscarbene complexes derived from other amino acids were also examined. The steric hindrance of the carbon atom of the substituent attached at the α-position of the amino acid residue appears to have a high impact on the activity of the catalyst. Thus, the use of complexes Val_2Ni and ILe_2Ni, with tertiary carbons in that position, resulted in a severe reduction in conversion (entries 13 and 14). Though the benzyl substituted complex (*i.e.*, Phe_2Ni) exhibited better activity (entry 15 *vs.* 13 and 14), the leucine-derived complex remains superior (entry 15 *vs.* 8). Similar trend is observed with the palladium complexes ILe_2Pd and Phe_2Pd (entries 16 and 17).

Table 1 Hydrosilylative reduction of acetophenone (**3a**) catalyzed by Ni and Pd biscarbene complexes[a]

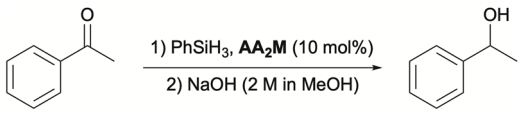

Entry	AA_2M	Solvent	T (°C)	Conv[b] (%)
1	Leu_2Pd	THF	30	39
2	Leu_2Pd	THF	50	51
3	Leu_2Pd	Toluene	30	13
4	Leu_2Pd	Toluene	50	75
5	Leu_2Ni	THF	30	18
6	Leu_2Ni	THF	50	84
7	Leu_2Ni	Toluene	30	0
8	Leu_2Ni	Toluene	50	91
9	Leu_2Ni	Dioxane	50	75
10	Leu_2Ni	DME	50	24
11	Leu_2Ni	$C_2H_4Cl_2$	50	82
12	Leu_2Ni	$C_2H_2Cl_4$	50	0
13	Val_2Ni	Toluene	50	28
14	ILe_2Ni	Toluene	50	1
15	Phe_2Ni	Toluene	50	78
16	ILe_2Pd	Toluene	50	12
17	Phe_2Pd	Toluene	50	45

[a] Reaction conditions: acetophenone (0.3 mmol), $PhSiH_3$ (0.36 mmol, 1.2 equiv.), AA_2M (0.03 mmol), 18 h. [b] Conversion determined by GC-MS.

We disclosed that half-sandwich nickel complexes of the **AANiCp** type are among the most efficient nickel catalysts for the hydrosilylative reduction of acetophenones described thus far, with **LeuNiCp** being the most prominent (average TOF up to 48 h^{-1} with acetophenone).[11] This catalyst surpassed the activity reported for other half-sandwich complexes of the formula [(NHC)NiCpX] (up to 2 h^{-1} with the same substrate),[13] or the most active pincer nickel complexes (up to 5 h^{-1}).[14] Furthermore, the reactions with **LeuNiCp** proceed without any additive/activator (*e.g.*, $NaHBEt_3$ or KO^tBu), which is generally required for other catalysts. Despite the greater electronic and coordinative unsaturation of Leu_2Ni (formally a d^8-ML_4 complex of 16 e^-, L a 2 e^- donor), the reactivity of this complex is lower (0.5 h^{-1}) than that of **LeuNiCp** (d^8-ML_5 of 18 e^-). However, as observed among the half-sandwich monocarbene family of complexes, the presence of the NHC-carboxylate chelating ligands in AA_2Ni complexes benefit their catalytic activity with ketones in comparison to other related bis(κ^2-C,O-NHC) nickel complexes, which are reported to be inactive in this reaction.[10]

With the optimized conditions in hand (Table 1, entry 8), a substrate scope of the reaction was explored by studying the hydrosilylation of various aryl and alkyl ketones to form the corresponding alcohols **4a–g** (Scheme 4). The *p*-chloro substituted acetophenone was reduced to give the alcohol (**4b**), albeit with a lower conversion (69%) compared to that of the unsubstituted compound. The *meta*-chloro aryl substitution did not impede the reaction, and good conversion was also obtained. However, the chloro substituent in the *ortho* position appears to sterically hamper the reaction. Substitution with an electron donating group, such as *p*-OMe, was somewhat deleterious to the reaction, as was observed with the analogous benzaldehyde, producing **4e** with 57% conversion. Aliphatic ketones were also susceptible to undergo this reaction and gave even better results. Cyclohexanone was fully converted into the alcohol (**4f**), and despite steric hindrance, *tert*-butylmethylketone also delivered the corresponding alcohol (**4g**) with 83% conversion.

We also tested the reaction with the α,β-unsaturated ketone 4-phenyl-3-buten-2-one (**3h**). Complete conversion occurred,

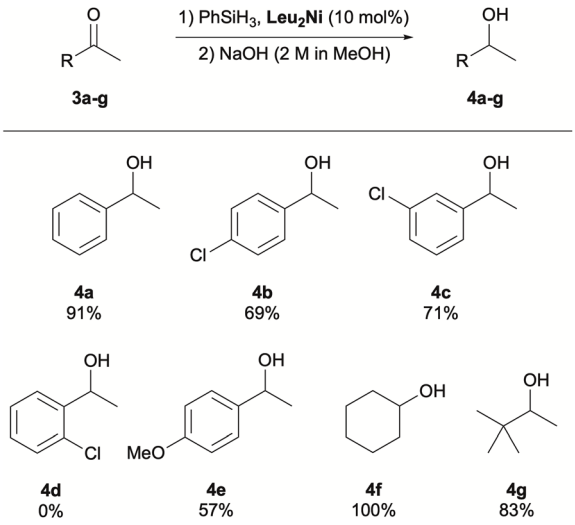

Scheme 4 Reaction conditions: ketone (0.3 mmol), $PhSiH_3$ (0.36 mmol, 1.2 equiv.), Leu_2Ni (0.03 mmol), toluene, 50 °C, 18 h. Conversion determined by GC-MS.

yielding a mixture of the allylic alcohol, **5h** the alkene reduction product **6h**, and the double hydrogenation product **7h** in a ratio 37 : 55 : 9 (Scheme 5). The lack of regioselectivity observed between the carbonyl group and the doble bond prompted us to increase the amount of the reducing agent. Thus, with 3 equivalents of $PhSiH_3$, the resulting mixture was enriched in the alcohol **7h** (72%), which could be separated through column chromatography from the ketone **6h** (28%). Chiral-HPLC analysis revealed a racemic mixture for the resulting secondary alcohols in all cases.

Computational analysis of stereo-electronic properties

The steric and electronic characteristics of a catalyst are fundamental parameters in catalyst design. Consequently, it was of interest to investigate these properties in $(\mathbf{MesAA})^-$ ligands. In previous work, we theoretically examined the bonding capabilities of related imidazole–carboxylate and imidazolium–carboxylate ligands.[15] Some chiral $(\mathbf{MesAA})^-$ ligands were also explored in preliminary form,[16] albeit at a different level of theory than that employed here. In the present study, the free $(\mathbf{MesAA})^-$ ligands (**AA** = Val, Leu, ILe, Phe) were analyzed using density functional theory (DFT). Geometry optimizations were carried out, and the resulting optimized structures are shown in Fig. S2. A molecular orbital analysis of the free ligands revealed that HOMO and HOMO-1 correspond to the in-phase and out-of-phase combinations of the in-plane lone pairs on the carboxylate oxygen atoms, whereas HOMO-3 represents a carbene-centered lone pair (Fig. S3). These orbitals are key contributors to the σ-coordination of the ligands to the metal center once the appropriate conformation is adopted. To evaluate the behavior of these orbitals upon coordination, the corresponding $\mathbf{AA_2Ni}$ complexes were optimized (Fig. 1). For each ligand, the molecular orbitals were examined using the fixed conformation obtained from the complex optimization. Coordination occurred through σ-donation from the HOMO (out-of-phase) and HOMO-3 (in-phase). The influence of the **AA** substituent on the energies of these orbitals is illustrated in Fig. 2. Ligands bearing alkyl substituents exhibit similar MO energies, whereas the incorporation of a phenyl group lowers these energies, indicating reduced σ-donor ability.

To obtain a more comprehensive picture of the electronic properties, the Tolman Electronic Parameters (TEP)[17] of these ligands were calculated using a modified version of Gusev's method.[18] Although this method was not originally developed for bidentate ligands, we have recently applied it to evaluate the electronic properties of bidentate carbenes.[19]

Following the same approach, $[Ni(CO)_2(\kappa^2\text{-}\mathbf{AA})]^-$ complexes featuring bidentate coordination were optimized (Table S1). The calculated ν_{CO} values for the $(\mathbf{MesAA})^-$ ligands fall within the 1960–1955 cm^{-1} range. These values are substantially lower than those reported for $[Ni(CO)_2(PR_3)_2]$[20] and $[Ni(CO)_2(\kappa^2$-C,O-(S)Poxim)][21] complexes (experimental ranges: 2045–1980 and 2042–2047 cm^{-1}, respectively), indicating that $(\mathbf{MesAA})^-$ ligands are stronger electron donors than either two phosphane ligands or the (S)Poxim bidentate ligand, the latter being *N*-phosphine oxide-substituted imidazole-2-ylidene species.[21] According to the extended Gusev analysis, ligands with alkyl substituents

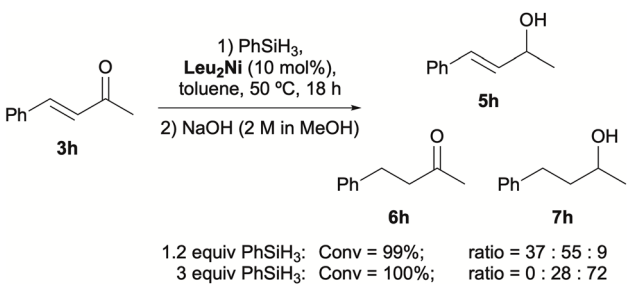

Scheme 5 Hydrosilylative reduction of 4-phenyl-3-buten-2-one (**3h**) catalyzed by Leu_2Ni.

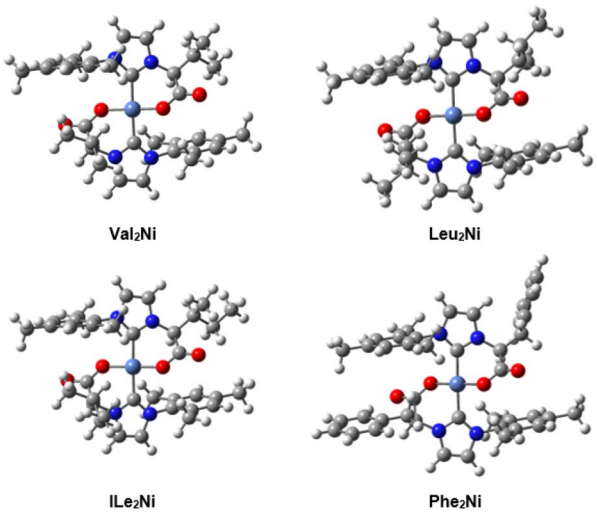

Fig. 1 Optimized structures of AA_2Ni complexes.

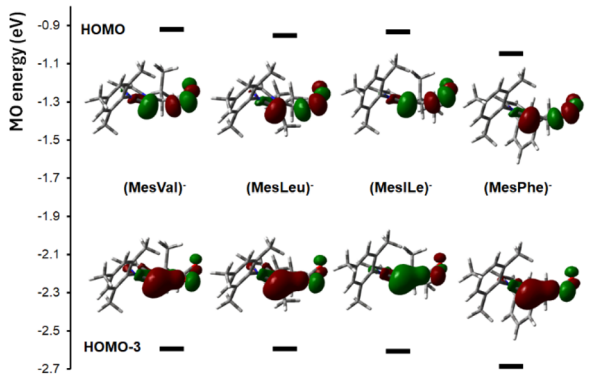

Fig. 2 Energies of HOMO and HOMO-3 in coordinated (**MesAA**)$^-$ ligands.

(Val, Leu, and ILe) exhibit TEP values below 1956 cm^{-1}, with (**MesLeu**)$^-$ showing the highest donor capacity. In contrast, incorporation of a phenyl substituent in (**MesPhe**)$^-$ reduces the electron-donating ability. Moreover, the calculated TEP values correlate well with the HOMO and HOMO-3 energies obtained for the (**MesAA**)$^-$ coordinated ligands, showing (**MesPhe**)$^-$ as the one having the orbitals with the lowest donor capacity and, accordingly, the highest TEP frequency (see Fig. S4).

Concerning the steric pressure exerted by the (**MesAA**)$^-$ ligands, the percent buried volume (%V_{bur}), calculated using the SambVca 2.1 software,[22] was obtained from the experimental X-ray structures of **AANiCp** complexes (Table S2).[11] The %V_{bur} values, which range from 45.0 to 46.7, allow differentiation of the steric properties associated with the various **AA** ligands. Ligands with alkyl substituents (Val, Leu, and ILe) exhibit the smallest %V_{bur} (*ca.* 45.1), whereas the ligand containing the phenyl substituent displays the greatest steric bulk. By combining the Tolman electronic parameter (TEP) values calculated for the [Ni(CO)$_2$(κ^2-**AA**)]$^-$ complexes with the steric parameters derived from the experimental X-ray structures of **AANiCp** complexes, a map of the electronic and steric characteristics of the (**MesAA**)$^-$ ligands was constructed (Fig. 3). The (**MesLeu**)$^-$ ligand, which corresponds to the most active catalyst

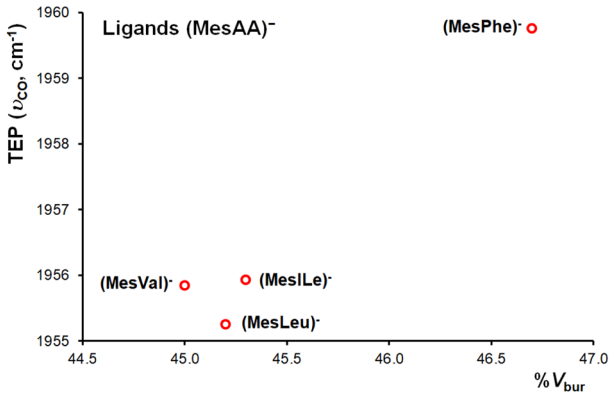

Fig. 3 Correlation between the TEP and %V_{bur} parameters of the (MesAA)$^-$ ligands in the AANiCp complexes.

in the studied reactions, exhibits the highest donor ability with an intermediate steric demand, among the alkyl substituted **AA** ligands, as measured by %V_{bur}.

Although a detailed mechanistic study has not been carried out, some key aspects of the reaction pathway were explored. First, we considered whether the mechanism might be initiated through dissociation of the carboxylate arm, thereby generating a vacant coordination site. From the optimized **Leu$_2$Ni** complex, which shows a good agreement between experimental and calculated structural parameters (Table S3), additional optimization of the species containing one uncoordinated carboxylate group (Fig. S5) was carried out. The dissociation process is endergonic by 46.5 kcal mol^{-1}. Since the uncatalyzed reaction between PhCHO and $PhSiH_3$ has a computed barrier of 41.0 kcal mol^{-1} (see profile in Fig. S6), carboxylate dissociation cannot represent the initial step of the catalytic cycle. Given that the system corresponds to a d^8-ML$_4$ complex, and that associative-type mechanisms are common for this class of species, we considered it instructive to evaluate the accessible coordination space in each complex as a function of the **AA** substituent. For this purpose, the AtomAccess program was employed.[23] This tool calculates the size of accessible coordination site within a complex, expressed as a percentage of solid angle. Table S4 presents the results obtained using experimental data from X-ray structures of the **AA$_2$Ni** complexes.[11] Although the differences are modest, the **Leu$_2$Ni** complex exhibits the highest percentage of accessible space (9.7%), whereas the complexes containing a tertiary carbon at the α-position of the amino acid (**MesVal** and **MesILe**) display lower values (7.6 and 7.1%, respectively). These results are consistent with the experimentally observed higher catalytic activity of the **Leu$_2$Ni** derivative. The experimental molecular structure of the **Leu$_2$Ni** complex shows two (**MesLeu**)$^-$ ligands forming six-membered metallacycles with boat conformations, oriented on opposite sides with respect to the molecular plane. A conformer in which these metallacycles are oriented on the same side of the molecular plane was optimized (Fig. S7). For this derivative, AtomAccess yields a larger percentage of accesible space (11.8%). Since this conformer lies only 8.7 kcal mol^{-1} above the **Leu$_2$Ni** complex, we propose that it may represent an initial state of the catalytic process.

Conclusions

We have developed a direct method to obtain the nickel bis-carbene complexes, **AA$_2$Ni**, in good yields through deprotonation with LDA, followed by *in situ* complexation with complete ligand substitution in [NiBr$_2$(dme)]. In addition, the family of palladium complexes, **AA$_2$Pd**, have been expanded with the leucine- and phenylalanine-derived NHC palladium compounds. The catalytic behavior of the **AA$_2$M** complexes in the hydrosilylative reduction of carbonyl compounds have been explored. Complex **Leu$_2$Ni** has shown good catalytic performances. Although it is less active with aldehydes than related complexes described in the literature, it is active with ketones, even when those complexes are reported to be inactive. As we previously observed with half-sandwich monocabene **AANiCp**

complexes,[11] the presence of a carboxylate group in NHC ligands appears beneficial for reactivity of the biscarbene **AA_2Ni** complexes as well. The DFT study carried out on the steric and electronic characteristics of the coordinated NHC-carboxylate ligands has allowed us to classify the (**MesLeu**)$^-$ ligand, from the complex with the highest catalytic activity, as one of the ligands exhibiting the greatest donor ability (as measured by its calculated TEP) while maintaining a medium steric demand (assessed through its $\%V_{bur}$). This confers to the metal center of the **Leu_2Ni** complex with the greatest degree of accessibility. These theoretical results identify small differences in several features (donor capability, $\%V_{bur}$ and metal site accessibility), which together contribute to supporting the experimental observation of **Leu_2Ni** complex as the most efficient catalytic candidate.

Author contributions

J. S.-G. and C. J. C.: investigation, validation, data curation. C. G.-A. and F. M.: methodology, formal analysis, supervision, funding acquisition. A. G. and J. C. F.: conceptualization, supervision, resources, funding acquisition, writing – original draft. All authors contributed to the writing – review and editing process of the manuscript.

Conflicts of interest

There are no conflicts to declare.

Data availability

The data supporting this article have been included as part of the supplementary information (SI). Supplementary information: synthetic and catalytic experimental details, characterization data, computational details, Tables S1–S5 and Fig. S1–S7. See DOI: https://doi.org/10.1039/d6ra00132g.

Acknowledgements

This work was supported by the Spanish MICINN (PID2020-114637GB-I00), the CAM (EPU-INV/2020/013) and UAH (GP2025-03). A. G. thanks the Centro de Servicios de Informatica y Redes de Comunicaciones (CSIRC), Universidad de Granada, for providing the computing time.

References

1 (*a*) H. Amouri, *Chem. Rev.*, 2023, **123**, 230–270; (*b*) K. Liu and R. Gust, *Coord. Chem. Rev.*, 2016, **329**, 191–213; (*c*) C. A. Smith, M. R. Narouz, P. A. Lummis, I. Singh, A. Nazemi, C.-H. Li and C. M. Crudden, *Chem. Rev.*, 2019, **119**, 4986–5056; (*d*) S. Bai and Y. F. Han, *Acc. Chem. Res.*, 2023, **56**, 1213–1227.

2 (*a*) M. N. Hopkinson, C. Richter, M. Schedler and F. Glorius, *Nature*, 2014, **510**, 485–496; (*b*) L. Mercs and M. Albrecht, *Chem. Soc. Rev.*, 2010, **39**, 1903–1912; (*c*) E. Peris, *Chem. Rev.*, 2018, **118**, 9988–10031.

3 (*a*) S. Díez-González, N. Marion and S. P. Nolan, *Chem. Rev.*, 2009, **109**, 3612–3676; (*b*) Q. Zhao, G. Meng, S. P. Nolan and M. Szostak, *Chem. Rev.*, 2020, **120**, 1981–2048; (*c*) S. S. Bera, G. Utecht-Jarzyńska, S. Yang, S. P. Nolan and M. Szostak, *Chem. Rev.*, 2025, **125**, 5349–5435.

4 (*a*) D. Janssen-Müller, C. Schlepphorst and F. Glorius, *Chem. Soc. Rev.*, 2017, **46**, 4845–4854; (*b*) H. Y. Wu, M. J. Koh, Z. C. Wang and S. L. Shi, *Angew. Chem., Int. Ed.*, 2025, **64**, e202503126.

5 (*a*) A. Neshat, P. Mastrorilli and A. M. Mobarakeh, *Molecules*, 2022, **27**, 95; (*b*) N. Mukherjee, B. Mondal, T. N. Saha and R. Maity, *Appl. Organomet. Chem.*, 2024, **38**, e6794.

6 A. A. Danopoulos, P. Cole, S. P. Downing and D. Pugh, *J. Organomet. Chem.*, 2008, **693**, 3369–3374.

7 A. Sánchez, J. Sanz-Garrido, C. J. Carrasco, F. Montilla, E. Álvarez, C. Gonzalez-Arellano, J. C. Flores and A. Galindo, *Inorg. Chim. Acta*, 2022, **537**, 120946–120952.

8 W. F. Li, H. M. Sun, Z. G. Wang, M. Z. Chen, Q. Shen and Y. Zhang, *J. Organomet. Chem.*, 2005, **690**, 6227–6232.

9 S. Shanmuganathan, O. Kühl, P. G. Jones and J. Heinicke, *Cent. Eur. J. Chem.*, 2010, **8**, 992–998.

10 S. Bertini and M. Albrecht, *Chimia*, 2020, **74**, 483–488.

11 J. Sanz-Garrido, A. Martin, C. Gonzalez-Arellano and J. C. Flores, *Dalton Trans.*, 2024, **53**, 1460–1468.

12 J. Sanz-Garrido, R. Andrés, C. Gonzalez-Arellano and J. C. Flores, *Adv. Synth. Catal.*, 2025, **367**, e202401289.

13 (*a*) L. Postigo and B. Royo, *Adv. Synth. Catal.*, 2012, **354**, 2613–2618; (*b*) L. P. Bheeter, M. Henrion, L. Brelot, C. Darcel, M. J. Chetcuti, J. B. Sortais and V. Ritleng, *Adv. Synth. Catal.*, 2012, **354**, 2619–2624; (*c*) M. Rocquin, V. Ritleng, S. Barroso, A. M. Martins and M. J. Chetcuti, *J. Organomet. Chem.*, 2016, **808**, 57–62; (*d*) F. Ulm, S. Shahane, L. Truong-Phuoc, T. Romero, V. Paapaefthimiou, M. Chessé, M. J. Chetcuti, C. Pham-Huu, C. Michon and V. Ritleng, *Eur. J. Inorg. Chem.*, 2021, 3074–3082.

14 (*a*) J. A. Fernández, J. M. García, P. Ríos and A. Rodríguez, *Eur. J. Inorg. Chem.*, 2021, 2993–2998; (*b*) A. Kumar, R. Gupta and G. Mani, *Organometallics*, 2023, **42**, 732–744.

15 (*a*) A. I. Nicasio, F. Montilla, E. Álvarez, R. P. Colodrero and A. Galindo, *Dalton Trans.*, 2017, **46**, 471–482; (*b*) P. Caballero, R. M. P. Colodrero, M. M. Conejo, A. Pastor, E. Álvarez, F. Montilla, C. J. Carrasco, A. I. Nicasio and A. Galindo, *Inorg. Chim. Acta*, 2020, **513**, 119923; (*c*) E. Borrego, A. I. Nicasio, E. Álvarez, F. Montilla, J. M. Córdoba and A. Galindo, *Dalton Trans.*, 2019, **48**, 8731–8739.

16 A. Sánchez, C. J. Carrasco, F. Montilla, E. Álvarez, A. Galindo, M. Pérez-Aranda, E. Pajuelo and A. Alcudia, *Pharmaceutics*, 2022, **14**, 748.

17 C. A. Tolman, *Chem. Rev.*, 1977, **77**, 313–348.

18 D. G. Gusev, *Organometallics*, 2009, **28**, 6458–6461.

19 C. J. Carrasco, F. Montilla, E. Álvarez and A. Galindo, *Inorg. Chem.*, 2025, **64**, 14871–14881.

20 C. A. Tolman, *J. Am. Chem. Soc.*, 1970, **92**, 2956–2965.

21 J. N. Leung, Y. Mondori, S. Ogoshi, Y. Hoshimoto and H. V. Huynh, *Inorg. Chem.*, 2024, **63**, 4344–4354.

22 (*a*) L. Falivene, R. Credendino, A. Poater, A. Petta, L. Serra, R. Oliva, V. Scarano and L. Cavallo, *Organometallics*, 2016, **35**, 2286–2293; (*b*) L. Falivene, Z. Cao, A. Petta, L. Serra, A. Poater, R. Oliva, V. Scarano and L. Cavallo, *Nat. Chem.*, 2019, **11**, 872–879.

23 G. K. Gransbury, S. C. Corner, J. G. C. Kragskow, P. Evans, H. M. Yeung, W. J. A. Blackmore, G. F. S. Whitehead, I. J. Vitorica-Yrezabal, N. F. Chilton and D. P. Mills, *ChemRxiv*. 2023, preprint, DOI: 10.26434/CHEMRXIV-2023-28Z84.